

RESEARCH ARTICLE

Influence of periaqueductal gray on other salience network nodes predicts social sensitivity

Myrthe G. Rijpma¹  | Winson F.Z. Yang^{1,2} | Gianina Toller¹ |
Giovanni Battistella¹ | Arseny A. Sokolov^{3,4,5} | Virginia E. Sturm¹ |
William W. Seeley¹ | Joel H. Kramer¹ | Bruce L. Miller¹ | Katherine P. Rankin¹

¹Department of Neurology, Memory and Aging Center, University of California San Francisco, San Francisco, California, USA

²Department of Psychological Sciences, College of Arts & Sciences, Texas Tech University, Lubbock, Texas, USA

³Département des Neurosciences Cliniques, Neuroscape@NeuroTech Platform, Service de Neuropsychologie et de Neuroréhabilitation, Centre Hospitalier Universitaire Vaudois (CHUV), Lausanne, Switzerland

⁴Wellcome Centre for Human Neuroimaging, Institute of Neurology, University College London, London, UK

⁵Department of Neurology, Neuroscape Center, University of California, San Francisco, California, USA

Correspondence

Myrthe G. Rijpma, Memory and Aging Center, Department of Neurology, University of California, San Francisco, 675 Nelson Rising Lane, Suite 190, San Francisco, CA 94158, USA.
Email: myrthe.rijpma@gmail.com.

Funding information

Larry L. Hillblom Foundation, Grant/Award Numbers: 2002/2j, 2014-A-004-NET; National Institutes of Health, Grant/Award Numbers: K23-AG021606, P01AG019724, P50AG023501, R01AG029577

Abstract

The intrinsic connectivity of the salience network (SN) plays an important role in social behavior, however the directional influence that individual nodes have on each other has not yet been fully determined. In this study, we used spectral dynamic causal modeling to characterize the effective connectivity patterns in the SN for 44 healthy older adults and for 44 patients with behavioral variant frontotemporal dementia (bvFTD) who have focal SN dysfunction. We examined the relationship of SN effective connections with individuals' socioemotional sensitivity, using the revised self-monitoring scale, an informant-facing questionnaire that assesses sensitivity to expressive behavior. Overall, average SN effective connectivity for bvFTD patients differs from healthy older adults in cortical, hypothalamic, and thalamic nodes. For the majority of healthy individuals, strong periaqueductal gray (PAG) output to right cortical ($p < .01$) and thalamic nodes ($p < .05$), but not PAG output to other central pattern generators contributed to sensitivity to socioemotional cues. This effect did not exist for the majority of bvFTD patients; PAG output toward other SN nodes was weak, and this lack of output negatively influenced socioemotional sensitivity. Instead, input to the left vAI from other SN nodes supported patients' sensitivity to others' socioemotional behavior ($p < .05$), though less effectively. The key role of PAG output to cortical and thalamic nodes for socioemotional sensitivity suggests that its core functions, that is, generating autonomic changes in the body, and moreover representing the internal state of the body, is necessary for optimal social responsiveness, and its breakdown is central to bvFTD patients' social behavior deficits.

KEYWORDS

behavioral variant frontotemporal dementia, dynamic causal modeling, periaqueductal gray, salience network, socioemotional sensitivity

This is an open access article under the terms of the Creative Commons Attribution-NonCommercial-NoDerivs License, which permits use and distribution in any medium, provided the original work is properly cited, the use is non-commercial and no modifications or adaptations are made.

© 2021 The Authors. *Human Brain Mapping* published by Wiley Periodicals LLC.

1 | INTRODUCTION

The function of a brain region is characterized in part by the dynamic patterns of connectivity that it has with other regions within and outside its neural network (Uddin, 2015). Studies investigating functional connectivity of the salience network (SN) demonstrate that the SN plays an important role in social behavior (Seeley, Menon, et al., 2007; Toller et al., 2018). However, functional connectivity analysis does not inform on causality or directionality of communication, even though information asymmetry plays a key role in brain network dynamics (Park & Friston, 2013). Dynamic causal modeling (DCM) yields better information on directional, or effective, connectivity within these networks. While earlier approaches of DCM applied only to task-based imaging, recent advances using spectral DCM have enabled investigators to use task-free functional imaging data as well, which can be used to model information flow among nodes of resting-state networks (Sharaev, Zavyalova, Ushakov, Kartashov, & Velichkovsky, 2016; van de Steen, Almgren, Razi, Friston, & Marinazzo, 2019). Since then, multiple studies have yielded novel insights in linking effective connectivity with behavior (Battistella & Simonyan, 2019; Cui et al., 2015; Li et al., 2020; Nicholson et al., 2017; Sokolov et al., 2018, 2020; Wei, Wu, Bi, & Baeken, 2020). Therefore, modeling causal and directional information flow in the SN and comparing patterns among neurotypical individuals and patients with social behavior deficits may be important to better understand how network dynamics are involved in social functioning, and how they change in disease.

The SN is predominantly comprised of regions in the limbic and paralimbic system, and plays an important role in integrating the homeostatic status of the body with information from other cognitive and affective systems. This facilitates interoceptive awareness and enables selection of appropriate behavioral responses based on the internal state of the body and external demands (Seeley, 2019; Seeley, Menon, et al., 2007). The SN has a particularly important role in managing socioemotional processes, which is evident from behavior deficits in behavioral variant frontotemporal dementia (bvFTD) patients, who develop striking impairments in socioemotional behavior (Seeley, Allman, et al., 2007; Zhou et al., 2010), and have focal neurodegeneration affecting the SN, including the dorsal ACC, anterior insula, periaqueductal gray (PAG), dorsomedial thalamus, and hypothalamus, with right stronger than left in early disease and extending throughout the frontal lobe as disease progresses (Rosen et al., 2002; Seeley, Menon, et al., 2007). SN functional connectivity also seems to play a role in healthy individuals' socioemotional sensitivity, as described by Toller et al. (2018). From anatomical and functional connectivity studies, Seeley et al. (2012b) assembled a working model of how SN nodes are expected to dynamically influence each other directionally, and how this system is expected to break down in bvFTD. However, network dynamics among all SN nodes have not been investigated; directional connectivity has been modeled for cortical SN nodes only (Bajaj & Killgore, 2021; Ham, Leff, de Boissezon, Joffe, & Sharp, 2013; Lamichhane & Dhamala, 2015). Additionally, the relation between SN network dynamics and behavior has thus far

been investigated for the construct of "emotional intelligence," but not for more specific social behavior constructs. One aspect of social function, sensitivity to others' subtle socioemotional cues, relies heavily on the formation of visceral responses to social signals. Previous work suggests that SN, and specifically the PAG, plays an important role in this (Toller et al., 2018). To regulate autonomic functions of the peripheral nervous system, the PAG and other "central pattern generators" (CPGs) (Sturm et al., 2018) generate stereotypical "fight," "flight," or "freeze" behavior (Grillner, 2006; Saper, 2002), and contribute to emotional responses more broadly. This function of the PAG could be especially important in social contexts by initiating social responses to subtle stimuli and providing a foundation for more complex social behaviors (Damasio & Carvalho, 2013; Motta, Carobrez, & Canteras, 2017).

In this study, we hypothesized that among healthy older adults, different patterns of effective PAG connectivity to other parts of the SN would influence the ability to detect subtle socioemotional cues, and that bvFTD patients with focal SN dysfunction would show different effective connectivity patterns than healthy individuals. Since bvFTD is associated with gray matter volume reduction and white matter disruptions (Whitwell, Avula, & Vemuri, 2010), we anticipate that structural lesions likely contribute to functional changes. However, the relationships among structure and function are highly complex in neurodegenerative disease (Bonakdarpour, Rogalski, Wang, Sridhar, & Hurley, 2017; Harrington et al., 2015) and in brain functioning in general (Damoiseaux & Greicius, 2009), and multimodal imaging would be required to disentangle the underlying cause of functional connectivity changes, which is beyond the scope of the current study. The goal of this study is to evaluate the impact of circuit disruption, independently of the structural changes that might contribute to this in neurodegenerative disease. To test these hypotheses, we used spectral DCM to identify the causal and asymmetric resting-state network dynamics of the SN, in combination with an observer-based measure of socioemotional sensitivity. We first modeled the average SN effective connectivity strength from resting-state data in older normal controls (ONC) and bvFTD patients, and investigated the differences between these groups. Next, we analyzed the relationship between each individual's connectivity estimates and their scores for social sensitivity. We examined whether PAG output toward other SN nodes or PAG input from other SN nodes predicted socioemotional sensitivity. Lastly, we used a clustering method to examine individual variation in patterns of SN effective connectivity among healthy older adults, and investigated how bvFTD patients mapped onto these commonly occurring patterns.

2 | METHODS

2.1 | Participants

Fifty-three patients with bvFTD were initially selected for this study and matched based on age and sex with 50 ONCs. For the ROI sphere size that was selected in this study, nine bvFTD patients' and six

ONCs' time series did not meet the model-based uncorrected $p < .05$ signal threshold (Zeidman, Jafarian, Corbin, et al., 2019), which indicated insufficient signal. They were therefore excluded from the selected sample. This resulted in inclusion of a final sample of 44 bvFTD patients and 44 ONCs. The bvFTD patients were diagnosed by a multidisciplinary team of neurologists, neuropsychologists and nurses after thorough assessment of neurological, neuropsychological and neuroimaging results using the FTDC criteria (Rascovsky et al., 2011). ONCs were only included when an unremarkable neurological exam was established, together with normal structural brain imaging results, and cognitive functioning within the normal range. All behavioral measures and informant ratings were obtained within an average number of 13 ± 23 days of the participants' fMRI scans. All participants were enrolled in research at the Memory and Aging Center (MAC) of the University of California San Francisco (UCSF). The Committee on Human Research at UCSF approved the study, and prior to testing all participants gave voluntary written informed consent, giving permission to use the collected data for analysis.

2.2 | Revised self-monitoring scale

The revised self-monitoring scale (RSMS) is a 13-item questionnaire that measures sensitivity to subtle socioemotional expressions of others and the tendency to modify behavior based on these social cues (Lennox & Wolfe, 1984). RSMS items are categorized into two subscales, of which one assesses the sensitivity to expressive behavior of others (EX), and includes statements such as "*The subject can usually tell when he/she said something inappropriate by reading it in the listener's eyes.*" We expected that a focus on the internal representation of social cues would best elucidate the contribution of the SN to social sensitivity, thus the RSMS EX was used as the primary outcome measure for the study. Informants (family members or friends who had known the participant for > 5 years) were asked to complete the measure, describing the study participant by rating items from "certainly, always true" to "certainly, always false" using a 6-point Likert scale.

The psychometric properties of the RSMS have been extensively investigated, and showed good internal reliability of all RSMS items combined, as well as for each subscale separately (Day, Schleicher, Unckless, & Hiller, 2002; Lennox & Wolfe, 1984; O'Cass, 2000). The instrument also reflects adequate test-retest reliability (Anderson, 1991), and correlates positively with scales that measure traits considered to benefit from strong self-monitoring, such as self-esteem (Miller, Omens, & Delvadia, 1991; Wolfe, Lennox, & Cutler, 1986), leadership skills (Ellis, 1988) and job performance (Day et al., 2002), and correlates negatively with traits such as shyness and social anxiety (Wolfe et al., 1986).

A number of studies that examine behavioral impairments in neurodegenerative disease showed that informant ratings on the RSMS are notably sensitive to social deficits associated specifically with bvFTD (Franklin et al., 2021; Shdo et al., 2016; Toller et al., 2018, 2020). In comparison to healthy individuals and other dementia

syndromes, bvFTD patients are evaluated to be particularly insensitive to social cues (Shdo et al., 2016; Toller et al., 2018). This insensitivity seems to accurately delineate disease severity as well, which reflects the RSMS' strong potential to contribute to differential diagnostics in clinical setting (Franklin et al., 2021; Toller et al., 2020). More important for the current study, multiple studies using different neuroimaging models have shown that RSMS scores are strongly correlated with the SN ICN in neurodegenerative disease. Shdo et al. (2016) showed a linear relationship between the RSMS and gray matter volume in structures part of the SN, Toller et al. (2021) showed evidence that higher RSMS scores predict white matter integrity between SN structures, and Toller et al. (2018) also found that functional connectivity strength in the SN is directly linked to higher RSMS. In summary, these studies reflect that the RSMS is a robust scale to differentiate bvFTD from other dementias, to assess disease severity for this syndrome, and to assess brain lesions caused by the disease, which is relevant to the goal of the current study.

2.3 | Image acquisition and preprocessing

Structural and functional scans were acquired using a 3 T Siemens Trio scanner at UCSF. A T1-weighted 3D magnetization prepared rapid gradient echo (MPRAGE) sequence was used to obtain the structural images, with parameters as follows: 160 sagittal slices, 1-mm thick, skip = 0 mm; repetition time = 2,300 ms; echo time = 2.98 ms; flip angle = 9°; field of view = 240×256 mm²; voxel size = 1 mm³; matrix size = 256×256 . Two-hundred and forty task-free functional MRI volumes were obtained over 8 min, during which participants were instructed to relax with their eyes closed, using a T2*-weighted gradient echo-planar imaging sequence (repetition time = 2,000 ms; echo time = 27 ms; flip angle = 80°; field of view = 230×230 mm²; inplane voxel size = 2.5 mm²; matrix size = 92×92). Functional imaging data were analyzed using Statistical Parametric Mapping (SPM)12 (The Wellcome Centre for Human Neuroimaging, n.d.) and the FMRIB Software Library (FSL) (Analysis Group FMRIB, n.d.) After discarding the first five volumes to allow for magnetic field stabilization, functional images were slice-time corrected, spatially realigned, co-registered to each participant's structural T1-weighted image, normalized to the Montreal Neurological Institute T1 (MNI) template using SPM segment, re-sampled at a voxel size of 2 mm³, and smoothed with a 6 mm full-width at half-maximum Gaussian kernel. Co-registered scans were visually inspected to identify scans with poor co-registration. Participants' scans that failed visual inspection through group consensus were excluded from the sample. An additional quality control step included inspection of motion during scanning. Since head motion can cause systematic but spurious correlations (Power, Barnes, Snyder, Schlaggar, & Petersen, 2012), only participants with a maximum translational movement of ≤ 3 mm, maximum rotational movement of $\leq 3^\circ$, and maximum displacement of ≤ 3 mm between functional volumes were included into the study. Mean root-mean-square of volume-to-volume changes in translational (in mm) and rotational (mean Euler angle)

movement were calculated since these metrics can be associated with functional network connectivity strength (Table 1). A CSF mask in the central portion of the lateral ventricles, and a white matter (WM) mask based on the highest probability in the FMRIB Software Library (FSL) tissue probability mask were used to extract mean CSF and WM time series.

2.4 | Spectral DCM with PEB

2.4.1 | Time series extraction

The preprocessed functional images were analyzed with a linear model containing a discrete cosine basis set with 58 functions with frequency characteristics of resting-state brain dynamics (0.0078–0.1 Hz) (Fransson, 2005; Kahan et al., 2014) including six head motion parameters as well as WM and CSF signals as covariates of no interest. We specified an F-contrast across the discrete cosine transforms (DCT), producing an SPM that identified regions exhibiting blood-oxygen-level-dependent (BOLD) fluctuations within the frequency band.

2.4.2 | ROI identification

To choose the most optimal ROI size, we calculated for each participant if the time series data of ROIs ranging from 2 to 8 mm in radius would pass the required signal threshold of $p < .05$ uncorrected within the model. This analysis of the data showed that over 25% of the sample had to be excluded when selecting ROI sizes smaller than 8 mm, whereas an ROI size of 8 mm had less detrimental effects of <15% exclusion. Thus, ROIs of 8 mm in radius were created using the MARSBAR toolbox for SPM (Brett, Anton, Valabregue, & Poline, 2002). This size selection was supported by careful examination of work by a number of research groups (Li et al., 2017; Sharaev et al., 2016; Sokolov et al., 2018, 2020, 2019), including spectral DCM validation

studies (Razi, Kahan, Rees, & Friston, 2015; Razi, Seghier, Zhou, Mccolgan, & Zeidman, 2018), and DCM studies that included subcortical structures such as the PAG (Roy et al., 2014; Sevel, Craggs, Price, Staud, & Robinson, 2015) which all yielded meaningful results when applying an ROI of 8 mm. Additionally, a study that investigated the direct influence of 4, 8, 12, or 16 mm ROI radius sizes in the default mode network (Almgren et al., 2018) found that results between ROI sizes were very similar. This suggests that ROI size selection does not have large influence on final results.

The 8 mm ROIs were centered around a previously published gray matter atrophy peak in the right ventral anterior insula (AI) (42, 17, –10) in early bvFTD (Seeley, 2010; Seeley et al., 2008), and a corresponding ROI was defined for the ventral AI in the left hemisphere (–42, 17, –10). In addition, using coordinates from two recent neuroimaging meta-analyses (Beissner, Meissner, Bar, & Napadow, 2013; Linnman, Moulton, Barmettler, Becerra, & Borsook, 2012), ROIs were defined in the bilateral dorsomedial thalamus (± 4 , –16, 8), bilateral hypothalamus (± 4 , –6, –10), and the bilateral amygdala (± 20 , –8, –12), and ROI coordinates for the midline structures, that is, the ACC (2, 10, 40) and the PAG (2, –32, –5) were placed in the right hemisphere to limit CSF inclusion. Thus, 10 ROIs were selected in total (see Figure S3 for an illustration). For each region, the principal eigenvariate was computed from the radius sphere centered on each regions' peak F -value and was adjusted for the motion confounds. Participants that had insufficient time-series signal at a threshold of $p < .05$ uncorrected in one or more ROIs were excluded from the data, which were 15 participants in total.

2.4.3 | First level model specification and inversion

To examine the causal and directional influence that SN nodes have on each other, we performed spectral DCM with resting-state data, in combination with the Parametric Empirical Bayes (PEB) framework in MATLAB (ver. R2019a) (Friston et al., 2016; Zeidman, Jafarian, Corbin, et al., 2019; Zeidman, Jafarian, Seghier,

TABLE 1 Demographics and clinical characteristics of participants ($N = 88$)

M (SD)	ONC	bvFTD	p value	R^2
N	44	44		
Age	65.2 (5.1)	61 (8)	.004	.09
Sex (M/F)	26/18	26/18	–	–
MMSE total score	29.3 (0.9)	23.9 (5.2)	<.001	.32
CDR global score	0 (0)	1.1 (0.6)	<.001	.62
CDR sum of boxes	0 (0)	6.1 (2.9)	<.001	.65
RSMS EX (max = 30)	20.5 (3.5)	9.5 (6.7)	<.001	.52
Average max translational movement (in mm)	0.8 (0.4)	0.9 (0.5)	.38	.009
Average max rotational movement (mean Euler angle)	0.6 (0.5)	1 (0.7)	.01	.07

Note: Statistical difference between bvFTD patients and ONCs was calculated using post hoc Dunnett–Hsu test.

Abbreviations: bvFTD, behavioral variant frontotemporal dementia; CDR, clinical dementia rating; EX, sensitivity to socioemotional expressiveness score; MMSE, Mini Mental State Examination; ONC, older normal controls; RSMS, revised self-monitoring scale.

et al., 2019). Spectral DCM is distinct from stochastic DCM, in that it uses second order statistics (cross-spectra) rather than the original time-series data. This has the consequence that the time-dependent random fluctuations that are important in resting-state data are not treated as stochastic noise. Rather, spectral DCM relies on a static assumption (deterministic), making it more suitable for analysis with resting-state data (Friston, Kahan, Biswal, & Razi, 2014; Razi et al., 2015). Since bvFTD patients have structural and functional network changes in the SN resulting from neurodegenerative disease, we expected the DCM models for bvFTD patients to differentiate from the ONC models. We therefore estimated the DCMs for ONC and bvFTD patients separately in all levels of our DCM analysis, that is, first, second, and third level.

DCM starts with model specification, which is often based on results from existing literature. Previous studies focused on the cortical nodes of the SN (e.g., bilateral vAI and ACC), but did not include subcortical nodes, and focused on healthy controls rather than patients with neurodegenerative disease (Bajaj & Killgore, 2021; Ham et al., 2013; Lamichhane & Dhamala, 2015). Since we had no prior knowledge of effective connectivity patterns in all SN nodes (i.e., cortical and subcortical), we specified a hypothesis-free fully connected model. In other words, our model estimated 100 possible connectivity parameters, including 10 recurrent self-connections from each node. This step was done for all bvFTD patients and ONCs based on their individual hemodynamic connectivity patterns within and between SN nodes (Zeidman, Jafarian, Corbin, et al., 2019). To find the optimal model fit in terms of tradeoff between accuracy and complexity, individual DCM models were estimated using Bayesian model inversion, which updates the model after every iteration, generating first-level DCM estimates for each individual for each effective node pair connection. To test the accuracy of the DCM model estimation, the percentage of variance explained by each model for each individual was calculated (Zeidman, Jafarian, Corbin, et al., 2019). The completed first-level PEB files can be accessed in Dryad public repository (Rijpm et al., 2021).

2.4.4 | Second level PEB analysis and Bayesian model averaging

We used the second level PEB framework to specify linear models representing each group's average effective connectivity and implemented Bayesian model averaging over this framework to account for model uncertainty. Effective connectivity matrices were generated with R Studio (ver. 1.2.5001) and display each group's node-to-node and self-connection (Figure 1). Positive values for the node-to-node connection represent activation, and negative values represent inhibition. For the self-connections this is reversed; positive values represent self-inhibition, and negative values represent self-activation (Zeidman, Jafarian, Seghier, et al., 2019). For the statistical assessment of significance of these probabilistic models, we used a posterior probability of $P_p = .99$, indicating very strong evidence (Kass and Raftery, 1995).

2.4.5 | Third level PEB analysis

Since structural and functional brain changes in bvFTD patients caused by neurodegenerative disease can have unwanted influence on model estimation, we modeled the second level PEB parameters of each individual at a third level, that is, a PEB of PEBs (Park, Friston, Pae, Park, & Razi, 2018; Zeidman, Jafarian, Seghier, et al., 2019) by generating (Bayesian) linear regression models that represent the difference for bvFTD compared with ONC. For the third level PEB, which requires greater statistical power to detect significant results than is required by the second level PEB analysis, we set a lower threshold of evidence at a posterior probability of $P_p = .74$, which is considered significant and reflects positive evidence (Kass and Raftery, 1995). Matrix figures were generated with R Studio (ver. 1.2.5001) and scripts for analysis and visualization are accessible in GitHub (Rijpm, 2021a, 2021b).

2.5 | Effective connectivity of the PAG in relation to the RSMS EX score

2.5.1 | PAG summary and single effective connection estimates predicting RSMS EX score

As a data reduction step, we calculated summary variables using SAS software (ver. 9.4) from each individuals' DCM connectivity parameter estimates by adding all effective node connections from the PAG to other SN nodes together (PAG output estimate) and adding all the effective connections from other SN nodes to the PAG (PAG input estimate). We derived separate cortical and subcortical input and output estimates, where the cortical estimates consisted of connections from the PAG to the ACC and bilateral vAI, and the subcortical estimates consisted of connections from the PAG to the thalamus, hypothalamus, and amygdala. The summary estimates were controlled for outliers. All subjects with a z-score of the summary estimates larger than 3 SDs from the mean were excluded. This resulted in exclusion of one bvFTD patient and one ONC. Using SAS software version 9.4, we first analyzed whether the PAG input and output summary estimates of the whole sample significantly predicted the RSMS EX score by running linear models controlling for age, rotational movement and diagnostic group, and repeated this step using the cortical and subcortical summary estimates. We also calculated the correlation between these subcortical and cortical summary estimates using Pearson's correlation coefficients for each diagnostic group separately. To further examine PAG effective connections with bilateral single SN nodes, we added effective connectivity estimates of same structures together (e.g., left and right amygdala nodes with the PAG) separately for input from and output to the PAG.

As a final exploratory analysis to confirm that we had not missed important predictors of RSMS occurring beyond the PAG connections, we also analyzed contribution across all single effective node connections to the RSMS EX score. Self-connections were excluded in this analysis, resulting in 90 comparisons in total. Due to the exploratory

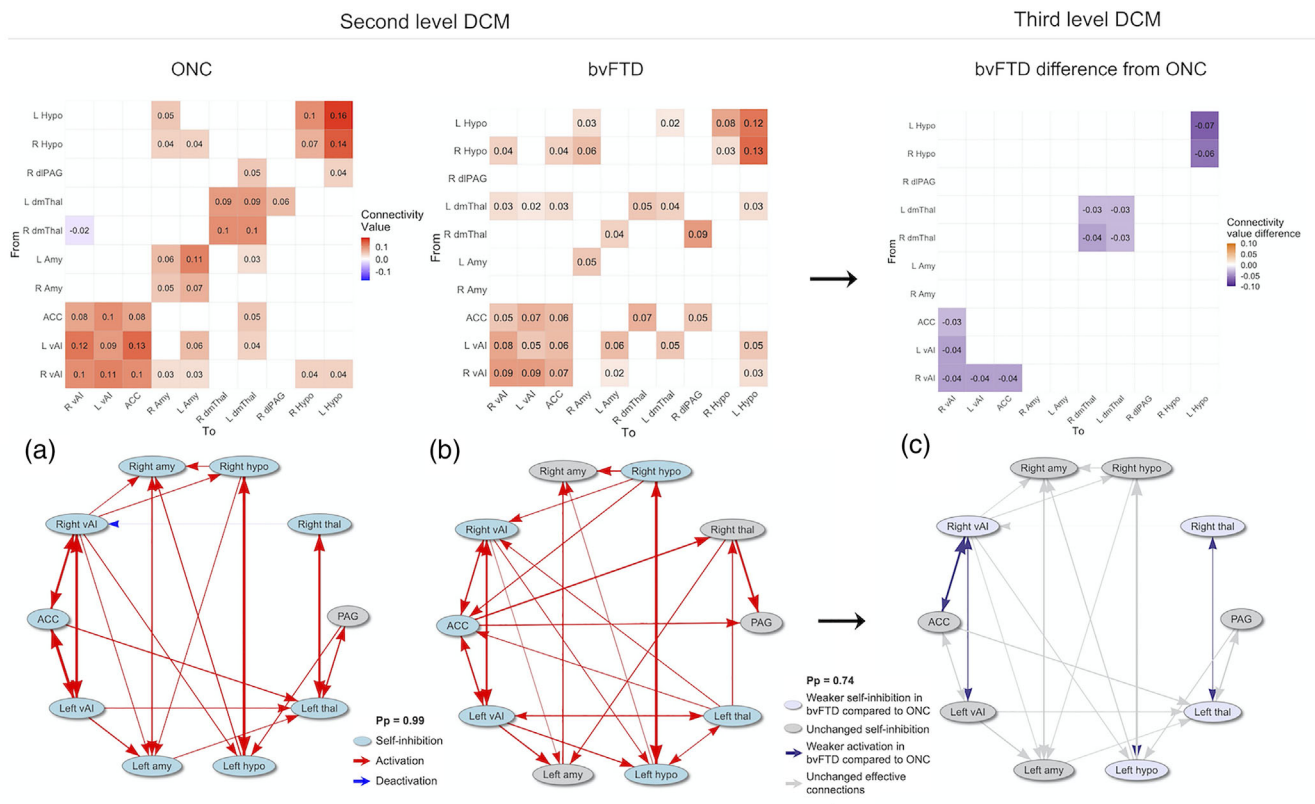


FIGURE 1 Matrices of mean effective connectivity of the ONC and bvFTD group and bvFTD compared with ONC, accompanied with schematic overviews of the effective connectivity results (thickness of lines equal the effective connectivity strength between node pairs). **(a)** At a $P_p = 0.99$, the ONC effective connectivity model shows reciprocal connections among the cortical vAI and ACC nodes. All subcortical bilateral counterparts are reciprocally connected as well. Self-connections are all self-inhibiting, except for the PAG. **(b)** At a $P_p = 0.99$, the bvFTD effective connectivity model shows reciprocal connections between the cortical SN nodes as well, as well as between the bilateral thalamic nodes. Self-connections are self-inhibiting in the bilateral hypothalamic nodes, the left thalamic node, the right vAI, and in the ACC, but are not significantly different in bilateral amygdala, right thalamus, and PAG. **(c)** The effective connectivity model of the bvFTD group compared with the effective connectivity model of the ONC group showed that at a $P_p = .74$ there was significantly weaker activation for the bvFTD group among (right) cortical nodes and subcortically between the bilateral thalamic nodes. Effective connectivity from the right to the left hypothalamus was significantly lower as well, and self-connections were less self-inhibiting in the right vAI, left hypothalamus and bilateral thalamic nodes. ACC, anterior cingulate cortex; amy, amygdala; bvFTD, behavioral variant frontotemporal dementia; hypo, hypothalamus; L, left; ONC, older normal controls; PAG, periaqueductal gray; Pp, posterior probability; R, right; thal, thalamus; vAI, ventral anterior insula

nature of this analysis and the large number of pairwise comparisons involved, the Benjamini–Yekutieli (B–Y) method was used as an FDR controlling procedure for multiple comparisons, with a threshold of $p < .00942$ for 90 comparisons (Narum, 2006).

2.5.2 | Cluster analysis with PAG summary estimates

To identify systematic variation (i.e., subgroups) among healthy older adults with respect to their patterns of effective connectivity, we performed in MATLAB (ver. 2019a) a k-means clustering analysis with the ONCs' cortical and subcortical summary variables. Selecting these summary variables (i.e., cortical and subcortical) enabled us to include all SN effective connections in an efficient

way. The appropriate number of clusters were identified based on the best average silhouette values per number of cluster groups and a visual check of the cluster silhouette plots. To identify how bvFTD patients' estimates for the cortical and subcortical summary variables differed from the ONC estimates, we then used the smallest pairwise Euclidean distance between centroids of the ONC clusters and the bvFTD estimates to establish cluster membership of the bvFTD group based on the ONC clusters. Next, we identified linear models using SAS software (ver. 9.4) for the ONC group and for the full sample to test whether cluster membership could predict performance on the RSMS EX score in health and in disease. Finally, we established whether a significant difference existed between ONC cluster membership and bvFTD cluster membership using a χ^2 analysis using SAS software (ver. 9.4) as well. Scripts for these analyses are available in GitHub (Rijpma, 2021c).

3 | RESULTS

3.1 | Demographics and clinical characteristics

The ONC group (65.2 ± 5.1) was statistically significantly older than the bvFTD group (61.0 ± 8.0 ; $p = .004$), however the average difference between groups was small (≈ 4 years) and therefore unlikely to have meaningful influences on the results. There were no significant sex differences between groups; in both groups 26 males and 18 females were included. Scores on the MMSE and CDR were significantly different between the bvFTD and ONC group, which was in line with the expected functional impairment for bvFTD patients. On the CDR global score, bvFTD patients scored 1.1 ± 0.6 , and on the CDR sum of boxes 6.1 ± 2.9 . For both CDR measures, the ONCs had a score of 0. On the MMSE, bvFTD patients scored 23.9 ± 5.2 , whereas ONC scored 29.3 ± 0.9 (Table 1).

3.2 | Group average effective connectivity strength of each SN node connection

3.2.1 | Effective connections in the ONC group

At a posterior probability of 99%, within-group effective connections for ONCs were all excitatory except for the right thalamus to right vAI connection, and a total of 27 effective connections were identified. This demonstrates that SN nodes generally have an activating influence on each other (Figure 1a). Similarly to the results in the DCM studies by Ham et al. (2013) and Lamichhane and Dhamala (2015), SN nodes were reciprocally connected among the cortical nodes. Additionally, the subcortical contralateral ROI (e.g., left with right amygdala) were all reciprocally connected as well. All self-connections showed statistically significant self-inhibition, except for the PAG node. Nodes with higher levels of self-connection are understood to be comparatively less responsive to inputs from other nodes (Zeidman, Jafarian, Corbin, et al., 2019), thus this result suggests that the PAG may be more responsive than other SN nodes. The percentage of explained variance reflected high accuracy of the DCM model for the ONC group; the average percentage of variance explained when fitting the DCM model-estimates to the cross-spectra was 68.50% ($SD = 22.30\%$), with a minimum of 41.21% and a maximum of 90.24%.

3.2.2 | Effective connections in the bvFTD group

At a Pp of 99%, there were 28 significant within-group effective connections for bvFTD patients, which were all excitatory (Figure 1b). The cortical nodes were all reciprocally connected, as well as the bilateral nodes of the hypothalamus. Self-connections were self-inhibiting in cortical, hypothalamic, and the left thalamus nodes, which indicates that these nodes are not very receptive for input from other nodes. The remaining nodes (i.e., amygdala, PAG, and right thalamus) were not significantly self-inhibiting or self-activating, suggesting that these

nodes are more receptive for input than the other SN nodes. Furthermore, the percentage of explained variance reflected that the estimated DCM model for the bvFTD group is highly accurate; the average explained variance when fitting the DCM model-estimates to the cross-spectra was 66.44% ($SD = 13.82\%$), with a minimum of 34.25% variance explained and a maximum of 94.85%.

3.2.3 | Differences in effective connectivity for bvFTD patients compared with ONCs

At a Pp of 74%, the bilateral effective connections between the insular nodes, and bilateral connections between the thalamic nodes were significantly lower for bvFTD patients compared with ONCs, as well as the reciprocal connection between the ACC and the right vAI, and effective connection from the right to the left hypothalamus (Figure 1c). Furthermore, self-connectivity in the right vAI, left hypothalamus, and bilateral thalamic nodes were significantly less self-inhibiting for bvFTD patients (compared with ONCs), which reflects that these nodes are more receptive for input from other SN nodes in bvFTD compared with ONC.

3.3 | Role of effective PAG connections in socioemotional sensitivity

3.3.1 | PAG summary estimates in relation to the RSMS EX score

Summary variables were calculated based on the entire sample (bvFTD and ONC) from individuals' DCM connectivity estimates. The summary variable of the entire sample representing PAG output toward other SN nodes significantly predicted higher RSMS EX score [$R^2 = .56$, $F(2,83) = 6.64$, $p = .012$], while the PAG input summary variable of the entire sample did not. The summary variables of the whole sample group were also divided into cortical and subcortical nodes. Output to cortical nodes significantly predicted higher RSMS EX score [$R^2 = .57$, $F(2,83) = 7.34$, $p = .0082$], but input to cortical nodes did not. Both PAG output and PAG input to subcortical nodes did not significantly predict the RSMS EX score, and when further evaluating this by using summary variables of single bilateral SN nodes (to and from the PAG), only the summary variable representing PAG output to the thalamic nodes predicted higher RSMS EX score [$R^2 = .16$, $F(2,83) = 5.50$, $p = .024$], and in ONCs only. All analyses were controlled for age, movement during scanning (mean Euler angle), and diagnostic group membership. See Figure S1 for all results.

3.3.2 | Single PAG effective connections in relation to the RSMS EX score

Next, we examined the contribution of each effective node-to-node connection that includes the PAG, separately for the ONC and the

bvFTD group. For the ONC group, PAG output to the ACC ($R^2 = .18$, $F = 6.76$, $p = .013$) and right vAI ($R^2 = .18$, $F = 6.24$, $p = .017$) significantly predicted higher RSMS EX score, as well as PAG output toward the left ($R^2 = .15$, $F = 4.69$, $p = .037$) and right thalamic nodes ($R^2 = .18$, $F = 6.24$, $p = .017$). Input from the right hypothalamus to the PAG ($R^2 = .21$, $F = 8.02$, $p = .0073$) predicted lower RSMS EX score. For the bvFTD group, PAG output toward the left vAI predicted higher RSMS EX scores ($R^2 = .23$, $F = 7.89$, $p = .0074$). These effects were controlled for age and movement during scanning (mean Euler angle).

$p < .01$. Next, a B-Y multiple comparison correction of $p < .00942$ was applied as a minimum threshold to gauge the statistical significance of results. Of these connections in ONCs, PAG output to the ACC ($R^2 = .16$, $F = 8.15$, $p = .0067$.) and right vAI ($R^2 = .16$, $F = 7.82$, $p = .0078$) remained statistically significant for higher RSMS EX scores, and input from the right hypothalamus to the PAG ($R^2 = .20$, $F = 9.97$, $p = .003$) remained significant for lower RSMS EX score. For the bvFTD group, no node pair significantly predicted RSMS EX scores after multiple comparison correction. See Figure S2 for the confidence limits of all analyses.

3.3.3 | All node pair effective SN connections as a predictor of RSMS EX score

We also conducted an exploratory analysis to identify whether separately for the ONC and bvFTD group effective node connections other than the connections with the PAG significantly contribute to the RSMS score. We included all 10 nodes for the ONC and bvFTD group in these analyses but excluded effective connectivity within each node (self-connections), resulting in 90 comparisons in total. Figure 2a,b display these 90 comparisons at a level of $p < .05$ and

3.3.4 | Cluster groups based on PAG output to cortical and subcortical SN nodes

By performing a k-means clustering analysis of the summary variables representing PAG output in the ONCs, we found that individuals could be split into three cluster groups based on differences in their patterns of connectivity. PAG input summary variables did not reflect any meaningful clusters. Compared with separation in two or four clusters (average silhouette values of .58 and .57, respectively), separation in three clusters yielded the highest average silhouette value

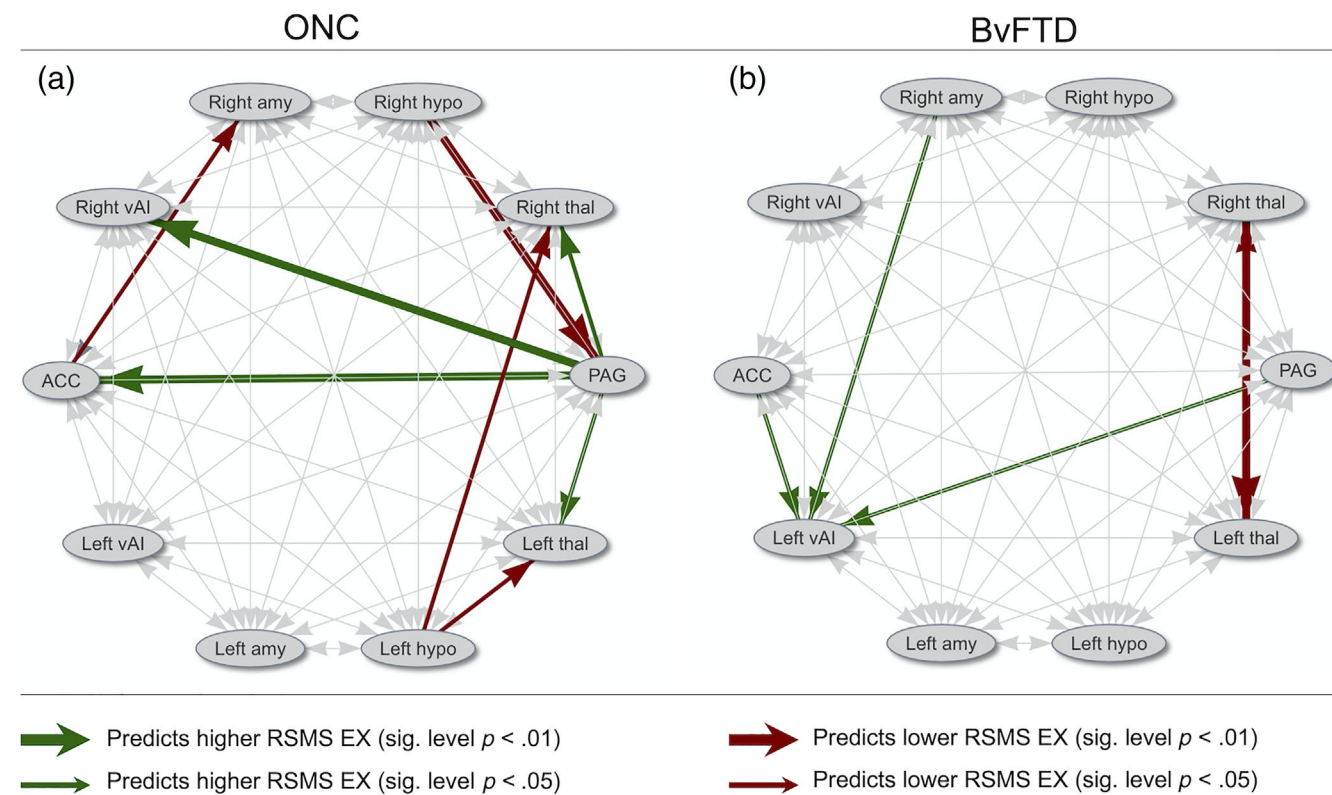


FIGURE 2 Schematic illustration of effective node connections that with a significance level of $p < .05$ or $p < .01$ predicted higher or lower RSMS EX scores, calculated separately for ONC and bvFTD patients (see Figure S2 for all effective node connections' confidence intervals in relation with the RSMS EX score). For the ONC group, PAG output to cortical and thalamic nodes positively predicted RSMS EX score, whereas input from the ACC, amygdala, and PAG to the left vAI positively predicted RSMS EX score for the bvFTD group. Mainly hypothalamic output had negative influence on the RSMS EX score for ONC, and bilateral thalamic connections for bvFTD patients. EX, expressive behavior; RSMS, revised self-monitoring scale

(.60). A visual check of the three-cluster analysis' silhouette plot showed that all data points in cluster group 3 have silhouette values above 0.8, and many data points in cluster groups 1 and 2 have

silhouette values around 0.7, which indicates that separation into three clusters is acceptable (see Figure 3d). Cluster group 1 (blue) exhibited low PAG output toward cortical and subcortical SN nodes.

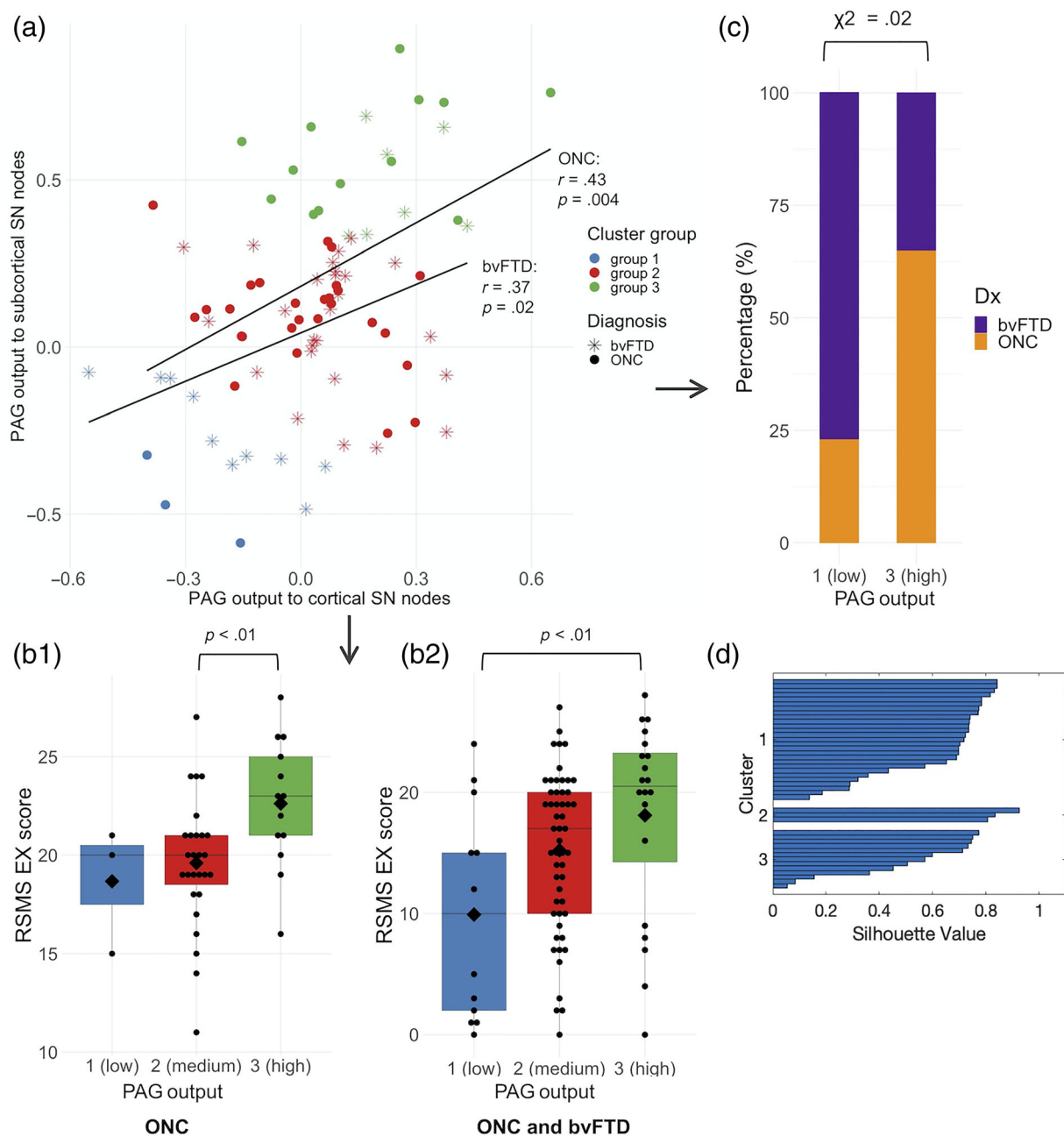


FIGURE 3 Individual differences in strength of PAG output predict RSMS EX score. (a) Comparing the summary estimates for PAG output to cortical nodes with PAG output to subcortical nodes yielded three different cluster groups in ONCs, of which group 1 (blue) showed weakest PAG output strength toward cortical and subcortical SN nodes, group 2 (red) showed medium output strength, and group 3 (green) showed most output strength toward cortical and subcortical SN nodes. (b1) When comparing RSMS EX scores of ONCs that belong to cluster group 3 (high PAG output) to cluster group 2 (medium PAG output), cluster group 3 performed significantly better on the RSMS EX scale than group 2. (b2) When comparing RSMS EX scores of the whole sample (i.e., ONCs and bvFTD patients combined), members of cluster group 3 performed significantly higher on the RSMS EX scale than members of cluster group 1. This suggests that stronger PAG output (toward cortical and subcortical SN nodes) increased socioemotional sensitivity, both in disease and in normal brain function. (c) By taking the χ^2 of cluster group membership per diagnostic group, bvFTD patients belonged significantly more to cluster group 1, and ONCs belonged significantly more to cluster group 3. This shows that compared with ONC, bvFTD patients belonged significantly more to the cluster group with weak PAG output and corresponding low RSMS EX scores. (d) Middle to high values on the silhouette plot shows that data can be safely divided into three clusters

Cluster group 2 (red) exhibited medium PAG output toward cortical and subcortical SN nodes, and cluster group 3 (green) exhibited high PAG output (Figure 3a). ONCs that belonged to cluster group 3 had significantly higher scores on the RSMS EX subscale than members of cluster group 2, $p < .01$ (Figure 3b1). There were no significant differences in RSMS EX score between cluster group 3 and 1, which is likely due to the small group size for group 1 (blue). When analyzing the whole sample (i.e., ONC and bvFTD), members of cluster group 3 scored significantly higher on the RSMS EX than members of cluster group 1, $p < .01$ (Figure 3b2) and there was a trend toward a significant difference between cluster group 3 and cluster group 2 ($p = .06$). Finally, bvFTD patients were significantly more likely to belong to cluster group 1, and ONCs were significantly more likely to belong to cluster group 3 ($\chi^2 = .02$), Figure 3c.

4 | DISCUSSION

This study clarifies for the first time the direction of information flow among subcortical and cortical nodes of the SN in neurotypicals, how that varies among individuals, how information flow in the SN is different for bvFTD patients compared with neurotypicals, and how this variation is linked to socioemotional sensitivity. Our results show that most healthy individuals show strong PAG output to other SN nodes, and that the strength of this directional information flow is a predictor of their ability to pick up on socioemotional cues. Specifically, PAG output to right cortical and thalamic nodes, but not PAG output to other central pattern generators, contributes to higher levels of socioemotional sensitivity in healthy individuals. Our results also show that on average bvFTD patients do not show the same SN effective connectivity patterns as older normal controls; directional activation is significantly decreased among cortical nodes, within hypothalamic nodes, and within thalamic nodes. Furthermore, we showed that for the majority of the bvFTD patients in our sample, PAG output toward other SN nodes was weak, and this breakdown in SN directional connectivity was a predictor of the diminished socioemotional sensitivity seen in these patients.

4.1 | Stronger PAG output to other SN nodes drives greater socioemotional sensitivity

Our study indicates that for older adults with healthy brain functioning, individuals with stronger PAG output to the cortical ACC, right vAI, and bilateral thalamic nodes were significantly more likely to be rated as socioemotionally sensitive by a close informant. Additionally, no other effective node connections seemed to contribute significantly to social sensitivity. This emphasizes the important role the PAG plays in picking up subtle socioemotional cues, and highlights a neural mechanism underlying individual variation in observable social behavior.

Animal models show that the PAG is situated at the interface of descending and ascending pathways between the peripheral nervous

system and higher order brain regions. The PAG is involved in many regulatory functions, but putatively its main role revolves around maintaining homeostatic balance for survival. For example, in conjunction with other CPGs such as the hypothalamus and amygdala, the PAG regulates autonomic responses such as “fight,” “flight,” and “freeze” behavior. The PAG can be functionally subdivided into different columns (Carrive, 1993; Linnman et al., 2012); the dorsolateral and lateral portion of the PAG evokes active coping strategies (“fight” and “flight”) through the sympathetic nervous system, whereas the ventrolateral portion generates opposite strategies of passive coping (“freeze”) through the parasympathetic system (Bandler, Keay, Floyd, & Price, 2006). The lateral and ventrolateral portion of the PAG receive afferent (ascending) connection that originate mainly from the spinal cord and the nucleus of the solitary tract (Bandler et al., 2006). Conversely, the dorsolateral column does not receive significant ascending input (Bandler et al., 2006). From the PAG, all columns project to the thalamus, although the ventrolateral column provides most input (Krout & Loewy, 2000). From there, the thalamus serves as a gateway for further projection to the insula and ACC (Benarroch, 2012; Cameron et al., 1995). Efferent (descending) connections of most subregions in the PAG are strongest with the superior colliculus, nucleus cuneiformis and the locus coeruleus of the midbrain, which in turn project to autonomic nuclei of the brainstem and spinal cord (Mantyh, 1983). Evidence from functional and structural imaging suggests that this system, originally delineated in animal models, seems to work similarly in humans (Linnman et al., 2012). These efferent and afferent loops allow us to both produce and sense changes in our internal milieu. Since the results in our study indicate that PAG influence on the thalamus, ACC, and vAI are the SN connections that most significantly contribute to socioemotional sensitivity, representation of internal states through the afferent pathway appears to be particularly important for picking up nuanced social behavior of others. However, our results do not rule out that the efferent pathway might play an additional role in social behavior by generating appropriate autonomic patterns in response to salient social cues.

In our study, ascending PAG output to bilateral thalamic nodes was a significant predictor of the level of socioemotional sensitivity as rated by observers. The role of the thalamus is to relay all incoming information from the periphery in a dynamic fashion, modulating the activation of other higher-order brain regions, depending on the contextual relevance (Basso, Uhlrich, & Bickford, 2005). This structure plays an important role in controlling the inflow of information to the vAI, and by extension downstream cortical regions (Craig, 1996). In the case of social cognition, this modulating function of the thalamus is likely performed via differential activation of neural pathways relevant to the consolidation of social information, and our results suggest that this mechanism might be important for sensing another person's subtle socioemotional cues. Ascending pathways play an important role in the parasympathetic nervous system, which relays internal cues from the periphery to the brain via afferent pathways (Craig, 1996), and the ascending connections from the PAG to the thalamus are part of this pathway (Krout & Loewy, 2000). Our ROI

was too large to definitively delineate the roles of the different PAG columns in socioemotional sensitivity in our analysis; however, our results do support the idea that socioemotional sensitivity may rely on parasympathetic systems, which relay internal cues from the periphery to the brain via afferent pathways. Our data do not rule out that sympathetic systems, which trigger physiological and behavioral responses via efferent pathways (Saper, 2002), may also contribute to sensitivity, thus these relationships require further clarification.

Our results also showed that PAG output toward the right vAI and ACC is beneficial to socioemotional sensitivity. The vAI is a major afferent hub for receiving and integrating autonomic signals from the body, and is the structure primarily responsible for bringing these bodily sensations to awareness (Craig, 2009; Damasio & Carvalho, 2013; Uddin, 2015). However, the vAI may play a dual role in which this sensitivity to one's own internal feeling state may convey greater awareness of the emotions of others in a social interaction. The significant role that the vAI plays in recognizing another's socioemotional state has previously been identified by Toller et al. (2018), who found that strong right vAI functional connectivity with other cortical and subcortical SN nodes supports more accurate social cue reading. The significant effect that dorsolateral PAG output toward the (right) vAI was found to have on socioemotional sensitivity in our study suggests that the afferent pathway that represents internal experiences contribute to social sensitivity. This communication from the PAG to the right vAI is most likely modulated by the thalamus, since no direct connections between the PAG and the vAI have been described (Vianna & Brandão, 2003). Furthermore, our finding that effective connectivity with only the right vAI was a predictor of socioemotional sensitivity corresponds with the autonomic imbalance known to exist between the left and right hemisphere, where the left hemisphere generates parasympathetic activation and the right hemisphere sympathetic activation (Craig, 2005; Sturm et al., 2018). This might indicate that social sensitivity is also supported by the efferent capacity to generate a sympathetic response that sequentially contributes to the afferent pathway.

Both the vAI and ACC structures possess neuroanatomically unique Von Economo and fork neurons (Allman et al., 2010; Seeley et al., 2012). Due to their longer axons, these neurons are thought to enable much more rapid signaling between the vAI/ACC and autonomic control structures compared with the more common pyramidal cells (Allman et al., 2010; Nimchinsky et al., 1999). This proposed anatomical advantage could aid rapid detection and synthesis of bodily signals by the vAI, and cognitive control regulation by the ACC, resulting in greater speed and precision of emotion-related behavioral responses (Craig, 2009; Evrard, 2018; Menon & Uddin, 2010; Stevens, Hurley, & Taber, 2011). Our study found that PAG output to the ACC contributes to socioemotional sensitivity. This suggests that the ACC may facilitate a more holistic representation of autonomic signals by modulating the transformation of the PAG's generated patterns into an emotional reaction, refining the intensity or quality of the behavioral response and thus lending greater subtlety to the awareness of the other's socioemotional cues.

PAG output toward the remaining CPGs, that is, the hypothalamus and the amygdala, did not contribute to socioemotional sensitivity in our study, nor did the output from these remaining CPGs to the SN. The main role of the CPGs is to generate autonomic signals and correct homeostasis, though the contribution of each CPG differs (Saper, 2002). While the PAG is mainly responsible for generating stereotypical autonomic patterns, the hypothalamus integrates a range of sensory information to maintain homeostasis of the body, and the amygdala alerts to the salience of environmental stimuli depending on one's motivational state (Benarroch, 2012; Cunningham & Brosch, 2012; Saper & Lowell, 2014). The extensive efferent connections that the CPGs have with nodes in the autonomic nervous system, and their lack of involvement in socioemotional sensitivity, suggests that social sensitivity might be more driven by afferent pattern recognition than by efferent pattern generation.

4.2 | bvFTD patients show altered PAG effective connectivity patterns predicting sensitivity

The relationship seen in ONC's was also present in bvFTDs, specifically that weaker PAG output in bvFTD patients predicted lower socioemotional sensitivity, and a disproportionate number of bvFTD patients fell in the group with the weakest PAG output. This finding extends the brain-behavior relationships we found in the neurotypical participants, supporting the idea that stronger directional PAG output contributes to greater social awareness. However, the specific effective connectivity patterns predicting behavior were altered in the bvFTD group. While in neurotypicals, having stronger PAG output toward bilateral thalamic and right cortical nodes was a predictor of socioemotional sensitivity, this effect did not exist for the bvFTD patient group. Also, while overall bvFTD patients were significantly less sensitive to socioemotional cues than the ONC group, a statistical trend was still seen in bvFTDs in which effective connections from the PAG, right amygdala, and ACC toward the left vAI predicted higher sensitivity to socioemotional cues. Disruption of normal PAG connections to thalamic and cortical nodes likely drove reduced sensitivity to socioemotional cues in these bvFTD patients. However, the enhanced left vAI contribution to socioemotional sensitivity might be a compensatory effect resulting from bvFTD-related disruption of other right-sided circuits that normally support this function (Seeley, 2008; Seeley et al., 2005). Disruption of right sided network connections could necessitate overfunctioning in the intact left vAI to bolster socioemotional sensitivity, though perhaps less effectively. Furthermore, the left vAI contributes to awareness of interoceptive processes, specifically for parasympathetic functioning (Guo et al., 2016). Therefore, its recruitment by bvFTD patients who retain some ability to correctly interpret another's socioemotional cues strengthens and extends our finding in the neurotypicals that socioemotional sensitivity seems to be supported mainly by the afferent pathway.

4.3 | Effective SN connections are different in bvFTD patients compared with ONCs

The overall strength of effective connections between SN nodes were on average lower in bvFTD patients than in ONCs. Effective connections between the contralateral vAI nodes and between the contralateral thalamic nodes, between the right vAI and ACC, and from the right to the left hypothalamus were significantly weaker. These findings are in line with earlier reports of SN disruption in bvFTD patients. For example, a study by Zhou et al. (2010) showed that compared with matched controls, bvFTD patients with mild disease progression (comparable to our sample) showed reduced SN connectivity strength in nodes corresponding with the vAI, ACC, hypothalamic, thalamic, and PAG nodes.

We also found that compared with ONCs, bvFTD patients showed significantly less self-inhibitory connections in the ACC, left vAI, bilateral thalamic nodes, and left hypothalamus. From a biological standpoint, effective self-connections can be interpreted as the excitatory-inhibitory balance within the region; high self-inhibition is thought to reflect low excitability (i.e., reactivity to input from other structures) whereas low self-inhibition reflects high excitability (Zeidman, Jafarian, Corbin, et al., 2019). This decreased self-inhibition in some SN nodes (i.e., higher excitability) in bvFTD patients may have emerged from mechanisms in the brain that compensate for disease-related network disruption, where a decrease in signal input could potentially lead to compensatory increased excitability in disrupted regions (Park & Reuter-Lorenz, 2009). The finding that only the right vAI shows significant changes in self-connection excitability supports this idea, since in the early stage right frontotemporal regions are more affected than the left in bvFTD (Seeley, 2008; Seeley et al., 2005).

4.4 | Limitations and conclusions

The objective of this study was to examine dynamic network connectivity in the SN and its relevance to social sensitivity. Because of the prominent role of the SN in social functioning, we selected only SN nodes for our DCM analyses, and along with healthy controls also included bvFTD patients, who have significant disease-related dysfunction in this network. This sample group enabled between-group comparisons, and the inclusion of lesion patients with clear abnormalities provided opportunity for more robust interpretation of the directionality of our connectivity results. This a priori selection of SN nodes, however, has the consequence that the role of effective connectivity patterns between other non-SN brain regions on socioemotional sensitivity remain unidentified in this study, and would be an appropriate next step for future research. Similarly to our selection of solely SN nodes, we set the prior hypothesis that socioemotional sensitivity would rely on dynamic connectivity to and from the PAG node specifically, limiting our investigation of the contribution of other SN nodes. We addressed this issue by running regression analyses for each

individual effective node connection, excluding the self-connections (i.e., 90 comparisons in total) to explore for any other meaningfully large contributions of SN node pairs to socioemotional sensitivity, though none emerged.

Another important consideration when interpreting this study is that structural connections between SN nodes are not directly represented in our results, since the effective connectivity modeled by the DCM approach is based only on functional activity. It is possible that influence of one node on the other is mediated by structural connections with a third node that was not included in the model. DCM methods that can incorporate structural connectivity information, such as regression DCM, could assess this in more detail (Frässle et al., 2021), and might be appropriate for a follow-up study. Additionally, our approach to characterize effective connectivity patterns among SN nodes yielded compelling results of how connectivity patterns in bvFTD are different from “typical” SN neural circuitry, but it provides no explanation of the cause of these changes. This question can only be addressed with an analytical approach that includes both structural and functional imaging data in a model, which was beyond the scope of this study, but is a relevant direction for future research. Finally, connections to and from the peripheral nervous system are important contributors to the function of the SN. However, dynamic connectivity between SN nodes and the periphery cannot be modeled with DCM. Though our results make a significant contribution to understanding network dynamics between nodes of the SN, interpretation of our results requires consideration of these analytical limitations.

In this study, we applied a novel approach by using effective connectivity DCM estimates to explore social behavior. This provides an example of how different analytical methods can be used to further expand our understanding of how activity in one brain node influences another, and how this forms observably different types of behavior. We showed that a relationship can be identified between effective connectivity and a very subtle type of behavior (detecting implicit socioemotional cues) that was measured using observer ratings (not rated by participants themselves), and was recognizable in nondisease models (healthy individuals) as well as in patients with focal neurodegeneration. This observation delivers substantial evidence that effective connections in the SN play an important role in behavior, and network mechanics should similarly be investigated in other cognitive domains as well. Additionally, expanded use of this approach with patients could extend our understanding of exactly how the function of intrinsically connected networks breaks down in neurologic disease, and whether this drives the wide variation in clinical symptoms frequently observed among individuals with the same syndrome.

ACKNOWLEDGMENTS

We would like to thank all patients, patients' caregivers and research volunteers for participating in this research project. We would also like to thank all research coordinators and fellows or postdocs at the UCSF Memory and Aging Center who supported us with data collection for this study.

CONFLICT OF INTEREST

The authors declare no conflicts of interest.

AUTHOR CONTRIBUTION

Myrthe G. Rijpma: Designed research plan, analyzed data, and wrote the article. **Winson F.Z. Yang:** Designed research plan, analyzed data, provided writing and editorial input on the article. **Gianina Toller:** Designed research plan, analyzed data, provided writing and editorial input on the article. **Giovanni Battistella:** Consulted on research design, contributed analytical tools, provided editorial input on the article. **Arseny A. Sokolov:** Consulted on research design, provided conceptual and technical consultation, provided editorial input on the article. **Virginia E. Sturm:** Provided conceptual and technical consultation and editorial input on the article. **William W. Seeley:** Provided conceptual and technical consultation and editorial input on the article. **Joel H. Kramer:** Provided participants and participant data and editorial input on the article. **Bruce L. Miller:** Provided participants and participant data, provided editorial input on the article. **Katherine P. Rankin:** Designed research plan, provided participant data, contributed to analytical tools, supported data analysis, and wrote the article.

ETHICS STATEMENT

All elements of this study were reviewed and approved by the UCSF Institutional Review Board (#14-14044). Prior to testing all participants gave voluntary written informed consent, giving permission to use the collected data for analysis.

DATA AVAILABILITY STATEMENT

All code used for analysis will be available at <https://github.com/MyrtheGwenRijpma/DCM>. Data matrices from individuals that support the imaging findings in this study will be available in the open access repository Dryad (<https://datadryad.org/stash/share>). Additional deidentified raw participant data cannot be placed in an open archive because it is not permitted under the study's IRB approval due to the sensitive nature of patients' data. However, all data is available to any interested research via a request submitted through a public-facing resource request portal at: <http://memory.ucsf.edu/resources/data>. Following a UCSF-regulated procedure, access will be granted to designated individuals in line with ethical guideline on the reuse of sensitive data. This would require submission of the Material Transfer Agreement, available at <https://icd.ucsf.edu/material-transfer-and-data-agreements>.

ORCID

Myrthe G. Rijpma  <https://orcid.org/0000-0001-7276-9175>

REFERENCES

- Allman, J. M., Tetreault, N. A., Hakeem, A. Y., Manaye, K. F., Semendeferi, K., Erwin, J. M., ... Hof, P. R. (2010). The von Economo neurons in fronto-insular and anterior cingulate cortex in great apes and humans. *Brain Structure & Function*, 214(5–6), 495–517. <https://doi.org/10.1007/s00429-010-0254-0>
- Almgren, H., van de Steen, F., Kühn, S., Razi, A., Friston, K., & Marinazzo, D. (2018). Variability and reliability of effective connectivity within the core default mode network: A multi-site longitudinal spectral DCM study. *NeuroImage*, 183, 757–768. <https://doi.org/10.1016/j.neuroimage.2018.08.053>
- Anderson, L. R. (1991). Test-retest reliability of the revised self-monitoring scale over a two-year period. *Psychological Reports*, 68(3), 1057–1058. <https://doi.org/10.2466/pr0.1991.68.3.1057>
- Bajaj, S., & Killgore, W. D. S. (2021). Association between emotional intelligence and effective brain connectome: A large-scale spectral DCM study. *NeuroImage*, 229, 1053–8119. <https://doi.org/10.1016/j.neuroimage.2021.117750>
- Bandler, R., Keay, K. A., Floyd, N., & Price, J. (2006). Central circuits mediating patterned autonomic activity during active vs. passive emotional coping. *Brain Research Bulletin*, 53(1), 95–104.
- Basso, M. A., Uhrlich, D., & Bickford, M. E. (2005). Cortical function: A view from the thalamus. *Neuron*, 45(4), 485–488. <https://doi.org/10.1016/j.neuron.2005.01.035>
- Battistella, G., & Simonyan, K. (2019). Top-down alteration of functional connectivity within the sensorimotor network in focal dystonia. *Neurology*, 92(16), 1–9. <https://doi.org/10.1212/WNL.0000000000007317>
- Beissner, F., Meissner, K., Bar, K.-J., & Napadow, V. (2013). The autonomic brain: An activation likelihood estimation meta-analysis for central processing of autonomic function. *Journal of Neuroscience*, 33(25), 10503–10511. <https://doi.org/10.1523/JNEUROSCI.1103-13.2013>
- Benarroch, E. E. (2012). Periaqueductal gray. *Neurology*, 78, 210–217.
- Bonakdarpour, B., Rogalski, E. J., Wang, A., Sridhar, J., & Hurley, R. S. (2017). Functional connectivity is reduced in early stage primary progressive aphasia when atrophy is not prominent. *Alzheimer Disease and Associated Disorders*, 31(2), 101–106. <https://doi.org/10.1097/WAD.000000000000193>
- Brett, M., Anton, J.-L., Valabregue, R., & Poline, J.-B. (2002). Region of interest analysis using an SPM toolbox. Presented at the 8th international conference on functional mapping of the human brain. *NeuroImage*, 16(2), 497.
- Cameron, A. A., Khan, I. A., Westlund, K. N., & Willis, W. D. (1995). The efferent projections of the periaqueductal gray in the rat: A phaseolus vulgaris-leucoagglutinin study. II. Descending projections. *Journal of Comparative Neurology*, 351(4), 585–601. <https://doi.org/10.1002/cne.903510408>
- Carrive, P. (1993). The periaqueductal gray and defensive behavior: Functional representation and neuronal organization. *Behavioural Brain Research*, 58(1–2), 27–47. [https://doi.org/10.1016/0166-4328\(93\)90088-8](https://doi.org/10.1016/0166-4328(93)90088-8)
- Craig, A. D. (1996). An ascending general homeostatic afferent pathway originating in lamina I. *Progress in Brain Research*, 107(1993), 225–242. [https://doi.org/10.1016/s0079-6123\(08\)61867-1](https://doi.org/10.1016/s0079-6123(08)61867-1)
- Craig, A. D. (2005). Forebrain emotional asymmetry: A neuroanatomical basis? *Trends in Cognitive Sciences*, 9(12), 566–571. <https://doi.org/10.1016/j.tics.2005.10.005>
- Craig, A. D. B. (2009). How do you feel—Now? The anterior insula and human awareness. *Nature Reviews Neuroscience*, 10, 59–70. <https://doi.org/10.1038/nrn2555>
- Cui, L.-B., Liu, J., Wang, L.-X., Li, C., Xi, Y.-B., Guo, F., ... Lu, H. (2015). Anterior cingulate cortex-related connectivity in first-episode schizophrenia: A spectral dynamic causal modeling study with functional magnetic resonance imaging. *Frontiers in Human Neuroscience*, 9(589), 1–10. <https://doi.org/10.3389/fnhum.2015.00589>
- Cunningham, W. A., & Brosch, T. (2012). Motivational salience: Amygdala tuning from traits, needs, values, and goals. *Current Directions in Psychological Science*, 21(1), 54–59. <https://doi.org/10.1177/0963721411430832>
- Damasio, A., & Carvalho, G. B. (2013). The nature of feelings: Evolutionary and neurobiological origins. *Nature Reviews Neuroscience*, 14(2), 143–152. <https://doi.org/10.1038/nrn3403>
- Damoiseaux, J. S., & Greicius, M. D. (2009). Greater than the sum of its parts: A review of studies combining structural connectivity and

- resting-state functional connectivity. *Brain Structure and Function*, 213(6), 525–533. <https://doi.org/10.1007/s00429-009-0208-6>
- Day, D. V., Schleicher, D. J., Unckless, A. L., & Hiller, N. J. (2002). Self-monitoring personality at work: A meta-analytic investigation of construct validity. *Journal of Applied Psychology*, 87(2), 390–401. <https://doi.org/10.1037/0021-9010.87.2.390>
- Ellis, R. J. (1988). Self-monitoring and leadership emergence in groups. *Personality and Social Psychology Bulletin*, 14(4), 681–693.
- Evrard, H. C. (2018). Von Economo and fork neurons in the monkey insula, implications for evolution of cognition. *Current Opinion in Behavioral Sciences*, 21, 182–190. <https://doi.org/10.1016/j.cobeha.2018.05.006>
- Franklin, H. D., Russell, L. L., Peakman, G., Greaves, C. V., Bocchetta, M., Nicholas, J., ... Finger, E. (2021). The revised self-monitoring scale detects early impairment of social cognition in genetic frontotemporal dementia within the GENFI cohort. *Alzheimer's Research & Therapy*, 13(127), 1–12.
- Fransson, P. (2005). Spontaneous low-frequency BOLD signal fluctuations: An fMRI investigation of the resting-state default mode of brain function hypothesis. *Human Brain Mapping*, 26(1), 15–29. <https://doi.org/10.1002/hbm.20113>
- Frässle, S., Harrison, S. J., Heinzle, J., Clementz, B. A., Tamminga, C. A., Sweeney, J. A., ... Stephan, K. E. (2021). Regression dynamic causal modeling for resting-state fMRI. *Human Brain Mapping*, 42(7), 2159–2180.
- Friston, K. J., Kahan, J., Biswal, B., & Razi, A. (2014). A DCM for resting state fMRI. *NeuroImage*, 94, 396–407. <https://doi.org/10.1016/j.neuroimage.2013.12.009>
- Friston, K. J., Litvak, V., Oswal, A., Razi, A., Stephan, K. E., Van Wijk, B. C. M., ... Zeidman, P. (2016). Bayesian model reduction and empirical Bayes for group (DCM) studies. *NeuroImage*, 128, 413–431. <https://doi.org/10.1016/j.neuroimage.2015.11.015>
- Grillner, S. (2006). Biological pattern generation: The cellular and computational logic of networks in motion. *Neuron*, 52(5), 751–766. <https://doi.org/10.1016/j.neuron.2006.11.008>
- Guo, C. C., Sturm, V. E., Zhou, J., Gennatas, E. D., Trujillo, A. J., Hua, A. Y., ... Seeley, W. W. (2016). Dominant hemisphere lateralization of cortical parasympathetic control as revealed by frontotemporal dementia. *Proceedings of the National Academy of Sciences of the United States of America*, 113(17), 2430–2439. <https://doi.org/10.1073/pnas.1509184113>
- Ham, T., Leff, A., de Boissezon, X., Joffe, A., & Sharp, D. J. (2013). Cognitive control and the salience network: An investigation of error processing and effective connectivity. *Journal of Neuroscience*, 33(16), 7091–7098. <https://doi.org/10.1523/JNEUROSCI.4692-12.2013>
- Harrington, D. L., Rubinov, M., Durgerian, S., Mourany, L., Reece, C., Koenig, K., ... Paulsen, J. S. (2015). Network topology and functional connectivity disturbances precede the onset of Huntington's disease. *Brain*, 138(8), 2332–2346. <https://doi.org/10.1093/brain/awv145>
- Kahan, J., Urner, M., Moran, R., Flandin, G., Marreiros, A., Mancini, L., ... Foltynie, T. (2014). Resting state functional MRI in Parkinson's disease: The impact of deep brain stimulation on “effective” connectivity. *Brain*, 137(4), 1130–1144. <https://doi.org/10.1093/brain/awu027>
- Kass, R. E., & Raftery, A. E. (1995). Bayes factors. *Journal of the American Statistical Association*, 90(430), 773–795. <https://doi.org/10.1080/01621459.1995.10476572>
- Krout, K. E., & Loewy, A. D. (2000). Periaqueductal gray matter projections to midline and intralaminar thalamic nuclei of the rat. *Journal of Comparative Neurology*, 424(1), 111–141. [https://doi.org/10.1002/1096-9861\(20000814\)424:1<111::AID-CNE9>3.0.CO;2-3](https://doi.org/10.1002/1096-9861(20000814)424:1<111::AID-CNE9>3.0.CO;2-3)
- Lamichhane, B., & Dhamala, M. (2015). The salience network and its functional architecture in a perceptual decision: An effective connectivity study. *Brain Connectivity*, 5(6), 362–370. <https://doi.org/10.1089/brain.2014.0282>
- Lennox, R. D., & Wolfe, R. N. (1984). Revision of the self-monitoring scale. *Journal of Personality and Social Psychology*, 46(6), 1349–1364.
- Li, G., Liu, Y., Zheng, Y., Li, D., Liang, X., Chen, Y., ... Shen, D. (2020). Large-scale dynamic causal modeling of major depressive disorder based on resting-state functional magnetic resonance imaging. *Human Brain Mapping*, 41(4), 865–881. <https://doi.org/10.1002/hbm.24845>
- Li, L., Li, B., Bai, Y., Liu, W., Wang, H., Leung, H. C., ... Tan, Q. (2017). Abnormal resting state effective connectivity within the default mode network in major depressive disorder: A spectral dynamic causal modeling study. *Brain and Behavior*, 7(7), 1–10. <https://doi.org/10.1002/brb3.732>
- Linnman, C., Moulton, E. A., Barmettler, G., Becerra, L., & Borsook, D. (2012). Neuroimaging of the periaqueductal gray: State of the field. *NeuroImage*, 60(1), 505–522. <https://doi.org/10.1016/j.neuroimage.2011.11.095>
- Mantyh, P. W. (1983). Connections of midbrain periaqueductal gray in the monkey. I. Descending efferent projections. *Journal of Neurophysiology*, 49(3), 567–581. <https://doi.org/10.1152/jn.1983.49.3.567>
- Menon, V., & Uddin, L. Q. (2010). Saliency, switching, attention and control: A network model of insula function. *Brain Structure and Function*, 214(5–6), 655–667. <https://doi.org/10.1007/s00429-010-0262-0>
- Miller, M. L., Omens, R. S., & Delvadia, R. (1991). Dimensions of social competence: Personality and coping style correlates. *Personality and Individual Differences*, 12(9), 955–964. [https://doi.org/10.1016/0191-8869\(91\)90185-E](https://doi.org/10.1016/0191-8869(91)90185-E)
- Motta, S. C., Carobrez, A. P., & Canteras, N. S. (2017). The periaqueductal gray and primal emotional processing critical to influence complex defensive responses, fear learning and reward seeking. *Neuroscience and Biobehavioral Reviews*, 76, 39–47. <https://doi.org/10.1016/j.neubiorev.2016.10.012>
- Narum, S. R. (2006). Beyond Bonferroni: Less conservative analyses for conservation genetics. *Conservation Genetics*, 7(5), 783–787. <https://doi.org/10.1007/s10592-005-9056-y>
- Nicholson, A. A., Friston, K. J., Zeidman, P., Harricharan, S., McKinnon, M. C., Densmore, M., ... Lanius, R. A. (2017). Dynamic causal modeling in PTSD and its dissociative subtype: Bottom-up versus top-down processing within fear and emotion regulation circuitry. *Human Brain Mapping*, 38(11), 5551–5561. <https://doi.org/10.1002/hbm.23748>
- Nimchinsky, E. A., Gilissen, E., Allman, J. M., Perl, D. P., Erwin, J. M., & Hof, P. R. (1999). A neuronal morphologic type unique to humans and great apes. *Proceedings of the National Academy of Sciences of the United States of America*, 96(9), 5268–5273. <https://doi.org/10.1073/pnas.96.9.5268>
- O'Casey, A. (2000). A psychometric evaluation of a revised version of the Lennox and Wolfe revised self-monitoring scale. *Psychology and Marketing*, 17(5), 397–419. [https://doi.org/10.1002/\(SICI\)1520-6793\(200005\)17:5<397::AID-MAR3>3.0.CO;2-D](https://doi.org/10.1002/(SICI)1520-6793(200005)17:5<397::AID-MAR3>3.0.CO;2-D)
- Park, D. C., & Reuter-Lorenz, P. (2009). The adaptive brain: Aging and neurocognitive scaffolding. *Annual Review of Psychology*, 60, 173–196. <https://doi.org/10.1146/annurev.psych.59.103006.093656>
- Park, H. J., & Friston, K. (2013). Structural and functional brain networks: From connections to cognition. *Science*, 342. <https://doi.org/10.1126/science.1238411>
- Park, H. J., Friston, K. J., Pae, C., Park, B., & Razi, A. (2018). Dynamic effective connectivity in resting state fMRI. *NeuroImage*, 180, 594–608. <https://doi.org/10.1016/j.neuroimage.2017.11.033>
- Power, J. D., Barnes, K. A., Snyder, A. Z., Schlaggar, B. L., & Petersen, S. E. (2012). Spurious but systematic correlations in functional connectivity MRI networks arise from subject motion. *NeuroImage*, 59(3), 2142–2154. <https://doi.org/10.1016/j.neuroimage.2011.10.018>
- Rascovsky, K., Hodges, J. R., Knopman, D., Mendez, M. F., Kramer, J. H., Neuhaus, J., ... Miller, B. L. (2011). Sensitivity of revised diagnostic criteria for the behavioural variant of frontotemporal dementia. *Brain*, 134(9), 2456–2477. <https://doi.org/10.1093/brain/awr179>
- Razi, A., Kahan, J., Rees, G., & Friston, K. J. (2015). Construct validation of a DCM for resting state fMRI. *NeuroImage*, 106, 1–14. <https://doi.org/10.1016/j.neuroimage.2014.11.027>

- Razi, A., Seghier, M. L., Zhou, Y., Mccolgan, P., & Zeidman, P. (2018). Large-scale DCMs for resting-state fMRI. *Network Neuroscience*, 1(3), 222–241. <https://doi.org/10.1162/NETN>
- Rijpm, M. G. (2021a). DCM second and third level visualization. *Zenodo*. <https://doi.org/10.5281/ZENODO.5081142>
- Rijpm, M. G. (2021b). Dynamic causal modeling PEB scripts. *Zenodo*. <https://doi.org/10.5281/ZENODO.5081128>
- Rijpm, M. G. (2021c). Dynamic causal modeling RSMS scripts. *Zenodo*. <https://doi.org/10.5281/ZENODO.5081135>
- Rijpm, M. G., Yang, W. F. Z., Toller, G., Battistella, G., Sokolov, A. A., Sturm, V. E., ... Rankin, K. P. (2021). Data from: Influence of periaqueductal gray on other salience network nodes predicts social sensitivity. *Dryad*.
- Rosen, H. J., Gorno-Tempini, M. L., Goldman, W. P., Perry, R. J., Schuff, N., Weiner, M., ... Miller, B. L. (2002). Patterns of brain atrophy in frontotemporal dementia and semantic dementia. *Neurology*, 58(2), 198–208. <https://doi.org/10.1212/WNL.58.2.198>
- Roy, M., Shohamy, D., Daw, N., Jepma, M., Wimmer, G. E., & Wager, T. D. (2014). Representation of aversive prediction errors in the human periaqueductal gray. *Nature Neuroscience*, 17(11), 1607–1612. <https://doi.org/10.1038/nn.3832>
- Saper, C. B. (2002). The central autonomic nervous system: Conscious visceral perception and autonomic pattern generation. *Annual Review of Neuroscience*, 25(1), 433–469. <https://doi.org/10.1146/annurev.neuro.25.032502.111311>
- Saper, C. B., & Lowell, B. B. (2014). The hypothalamus. *Current Biology*, 24(23), R1111–R1116. <https://doi.org/10.1016/j.cub.2014.10.023>
- Seeley, W. W. (2008). Selective functional, regional, and neuronal vulnerability in frontotemporal dementia. *Current Opinion in Neurology*, 21(6), 701–707. <https://doi.org/10.1097/WCO.0b013e3283168e2d>
- Seeley, W. W. (2010). Anterior insula degeneration in frontotemporal dementia. *Brain Structure and Function*, 214(5), 465–475. <https://doi.org/10.1007/s00429-010-0263-z>
- Seeley, W. W. (2019). The salience network: A neural system for perceiving and responding to homeostatic demands. *The Journal of Neuroscience: The Official Journal of the Society for Neuroscience*, 39(50), 9878–9882. <https://doi.org/10.1523/JNEUROSCI.1138-17.2019>
- Seeley, W. W., Allman, J. M., Carlin, D. A., Crawford, R. K., Macedo, M. N., Greicius, M. D., ... Miller, B. L. (2007a). Divergent social functioning in behavioral variant frontotemporal dementia and Alzheimer disease: Reciprocal networks and neuronal evolution. *Alzheimer Disease and Associated Disorders*, 21(4), 50–57.
- Seeley, W. W., Bauer, A. M., Miller, B. L., Gorno-Tempini, M. L., Kramer, J. H., Weiner, M., & Rosen, H. J. (2005). The natural history of temporal variant frontotemporal dementia. *Neurology*, 264(8), 1384–1390.
- Seeley, W. W., Crawford, R., Rascofsky, K., Kramer, J. H., Weiner, M., Miller, B. L., & Gorno-Tempini, M. L. (2008). Frontal paralimbic network atrophy in very mild behavioral variant frontotemporal dementia. *Archives of Neurology*, 65(2), 249–255. <https://doi.org/10.1001/archneurol.2007.38>
- Seeley, W. W., Menon, V., Schatzberg, A. F., Keller, J., Glover, G. H., Kenna, H., ... Greicius, M. D. (2007b). Dissociable intrinsic connectivity networks for salience processing and executive control. *The Journal of Neuroscience*, 27(9), 2349–2356. <https://doi.org/10.1523/JNEUROSCI.5587-06.2007>
- Seeley, W. W., Merkle, F. T., Gaus, S. E., Craig, A. D., Allman, J. M., & Hof, P. R. (2012a). Distinctive neurons of the anterior cingulate and frontoinsula cortex: A historical perspective. *Cerebral Cortex*, 22(2), 245–247. <https://doi.org/10.1093/cercor/bhr005>
- Seeley, W. W., Zhou, J., & Kim, E.-J. (2012b). Frontotemporal dementia: What can the behavioral variant teach us about human brain organization? *The Neuroscientist*, 18(4), 373–385. <https://doi.org/10.1177/1073858411410354>
- Sevel, L. S., Craggs, J. G., Price, D. D., Staud, R., & Robinson, M. E. (2015). Placebo analgesia enhances descending pain-related effective connectivity: A dynamic causal modeling study of endogenous pain modulation. *Journal of Pain*, 16(8), 760–768. <https://doi.org/10.1016/j.jpain.2015.05.001>
- Sharaev, M. G., Zavyalova, V. V., Ushakov, V. L., Kartashov, S. I., & Velichkovsky, B. M. (2016). Effective connectivity within the default mode network: Dynamic causal modeling of resting-state fMRI data. *Frontiers in Human Neuroscience*, 10(14), 1–9. <https://doi.org/10.3389/fnhum.2016.00014>
- Shdo, S. M., Ranasinghe, K. G., Gola, K. A., Mielke, C. J., Sukhanov, P. V., Miller, B. L., & Rankin, K. P. (2016). Deconstructing empathy: Neuroanatomical dissociations between affect sharing and prosocial motivation using a patient lesion model. *Neuropsychologia*, 116, 1–10. <https://doi.org/10.1016/j.neuropsychologia.2017.02.010>
- Sokolov, A. A., Ryylin, P., Zeidman, P., Pavlova, M. A., Friston, K. J., & Erb, M. (2018). Structural and effective brain connectivity underlying biological motion detection. *Proceedings of the National Academy of Sciences*, 115(51), E12034–E12042. <https://doi.org/10.1073/pnas.1812859115>
- Sokolov, A. A., Zeidman, P., Erb, M., Pollick, F. E., Fallgatter, A. J., Ryylin, P., ... Pavlova, M. A. (2020). Brain circuits signaling the absence of emotion in body language. *Proceedings of the National Academy of Sciences of the United States of America*, 117(34), 20868–20873. <https://doi.org/10.1073/pnas.2007141117>
- Sokolov, A. A., Zeidman, P., Erb, M., Ryylin, P., Pavlova, M. A., & Friston, K. J. (2019). Linking structural and effective brain connectivity: Structurally informed parametric empirical Bayes (si-PEB). *Brain Structure and Function*, 224, 205–217. <https://doi.org/10.1007/s00429-018-1760-8>
- Stevens, F. L., Hurley, R. A., & Taber, K. H. (2011). Anterior cingulate cortex: Unique role in cognition and emotion. *Journal of Neuropsychiatry and Clinical Neurosciences*, 23(2), 121–125. <https://doi.org/10.1176/jnp.23.2.jnp121>
- Sturm, V. E., Brown, J. A., Hua, A. Y., Lwi, S. J., Zhou, J., Kurth, F., ... Seeley, W. W. (2018). Network architecture underlying basal autonomic outflow: Evidence from frontotemporal dementia. *Journal of Neuroscience*, 38(42), 8943–8955. <https://doi.org/10.1523/JNEUROSCI.0347-18.2018>
- Toller, G., Brown, J., Sollberger, M., Shdo, S. M., Bouvet, L., Sukhanov, P., ... Rankin, K. P. (2018). Individual differences in socioemotional sensitivity are an index of salience network function. *Cortex*, 103, 211–223. <https://doi.org/10.1016/j.cortex.2018.02.012>
- Toller, G., Mandelli, M. L., Cobigo, Y., Rosen, H. J., Kramer, J. H., Miller, B. L., ... Rankin, K. P. (2021). Right uncinate fasciculus supports socioemotional sensitivity in health and neurodegenerative disease. *Unpublished manuscript*.
- Toller, G., Ranasinghe, K., Cobigo, Y., Staffaroni, A., Appleby, B., Brushaber, D., ... Rankin, K. (2020). Revised self-monitoring scale: A potential endpoint for frontotemporal dementia clinical trials. *Neurology*, 94(22), e2384–e2395. <https://doi.org/10.1212/WNL.0000000000009451>
- Uddin, L. Q. (2015). Salience processing and insular cortical function and dysfunction. *Nature Reviews Neuroscience*, 16(1), 55–61. <https://doi.org/10.1038/nrn3857>
- van de Steen, F., Almgren, H., Razi, A., Friston, K., & Marinazzo, D. (2019). Dynamic causal modelling of fluctuating connectivity in resting-state EEG. *NeuroImage*, 189, 476–484. <https://doi.org/10.1016/j.neuroimage.2019.01.055>
- Vianna, D. M. L., & Brandão, M. L. (2003). Anatomical connections of the periaqueductal gray: Specific neural substrates for different kinds of fear. *Brazilian Journal of Medical and Biological Research*, 36(5), 557–566. <https://doi.org/10.1590/S0100-879X2003000500002>
- Wei, L., Wu, G. R., Bi, M., & Baeken, C. (2020). Effective connectivity predicts cognitive empathy in cocaine addiction: A spectral dynamic

- causal modeling study. *Brain Imaging and Behavior*, 15(3), 1553–1561. <https://doi.org/10.1007/s11682-020-00354-y>
- Whitwell, J. L., Avula, R., & Vemuri, P. (2010). Gray and white matter water diffusion in the syndromic variants of frontotemporal dementia. *Neurology*, 74(16), 1279–1287.
- Wolfe, R. N., Lennox, R. D., & Cutler, B. L. (1986). Getting along and getting ahead. Empirical support for a theory of protective and acquisitive self-presentation. *Journal of Personality and Social Psychology*, 50(2), 356–361. <https://doi.org/10.1037/0022-3514.50.2.356>
- Zeidman, P., Jafarian, A., Corbin, N., Seghier, M. L., Razi, A., Price, C. J., & Friston, K. J. (2019a). A guide to group effective connectivity analysis, part 1: First level analysis with DCM for fMRI. *NeuroImage*, 200, 174–190. <https://doi.org/10.1016/j.neuroimage.2019.06.031>
- Zeidman, P., Jafarian, A., Seghier, M. L., Litvak, V., Cagnan, H., Cathy, J., ... Wing, W. (2019b). A tutorial on group effective connectivity analysis, part 2: Second level analysis with PEB 1 Introduction. *NeuroImage*, 200, 12–25.
- Zhou, J., Greicius, M. D., Gennatas, E. D., Growdon, M. E., Jang, J. Y., Rabinovici, G. D., ... Seeley, W. W. (2010). Divergent network connectivity changes in behavioural variant frontotemporal dementia and Alzheimer's disease. *Brain*, 133(5), 1352–1367. <https://doi.org/10.1093/brain/awq075>

SUPPORTING INFORMATION

Additional supporting information may be found in the online version of the article at the publisher's website.

How to cite this article: Rijpma, M. G., Yang, W. F. Z., Toller, G., Battistella, G., Sokolov, A. A., Sturm, V. E., Seeley, W. W., Kramer, J. H., Miller, B. L., & Rankin, K. P. (2022). Influence of periaqueductal gray on other salience network nodes predicts social sensitivity. *Human Brain Mapping*, 43(5), 1694–1709. <https://doi.org/10.1002/hbm.25751>